

Fine, I'll Merge It Myself: A Multi-Fidelity Framework for Automated Model Merging

Guinan Su¹

Jonas Geiping^{1,2,3}

¹Max Planck Institute for Intelligent Systems

²ELLIS Institute Tübingen, ³Tübingen AI Center

Abstract

Large language models (LLMs) have steadily advanced in capability, but their development requires extensive proprietary datasets and computational resources. One way to efficiently supplement capabilities with is model merging, which offers a promising alternative by combining multiple models without retraining. However, current merging approaches rely on manually-designed strategies for merging hyperparameters, limiting the exploration of potential model combinations and requiring significant human effort. We propose an Automated Model Merging Framework that enables fine-grained exploration of merging strategies while reducing costs through multi-fidelity approximations. We support both single and multi-objective optimization and introduce two novel search spaces: layer-wise fusion (LFS) and depth-wise integration (DIS). Evaluating across a number of benchmarks, we find that the search autonomously finds 1) Merges that further boost single-objective performance, even on tasks the model has already been finetuned on, and 2) Merges that optimize multi-objective frontiers across tasks. Effective merges are found with limited compute, e.g. within less than 500 search steps. The code is available at.¹

1 Introduction

Recent advancements in large-scale pre-trained models like GPT-4 [OpenAI et al., 2023], LLaMA [Touvron et al., 2023], DALL-E [Ramesh et al., 2021], and Imagen [Saharia et al., 2022] have demonstrated remarkable capabilities across diverse domains. Within Large Language Models (LLMs), specialized models have emerged excelling in specific tasks such as instruction following [Xu et al., 2023, Jiang et al., 2023, Bi et al., 2024], code generation [Luo et al., 2023b, Guo et al., 2024, Zhu et al., 2024], and mathematical problem-solving [Luo et al., 2023a]. However, developing models with comprehensive capabilities remains challenging. A straightforward solution would be to combine training data from specialized domains for retraining or finetuning. However, this data-centric approach faces practical limitations: it requires substantial resources, and many training datasets remain proprietary or restricted. Researchers have turned to model-centric approaches that enhance capabilities by leveraging existing pre-trained models without training or data access.

Model merging has emerged as a promising solution in this space. Beginning with simple weight averaging for models sharing initialization [Utans, 1996], more advanced parameter-based techniques were subsequently developed. Parameter-based methods like Task Arithmetic [Ilharco et al., 2022] and SLERP [White, 2016] advanced the field through parameter difference computation and spherical interpolation. Recent sparsity-based approaches like TIES-Merging [Yadav et al., 2024] and DARE [Yu et al., 2024] leverage neural network over-parametrization, using magnitude-based selection and rescaling to further improve merging effectiveness. However, these model merging methods rely on manually-tuned hyperparameters, applied uniformly across the entire model, which makes finding optimal solutions challenging.

¹<https://github.com/Guinan-Su/auto-merge-llm>

In this paper, we propose a **cost-efficient automated framework** for model merging. Our approach leverages low-fidelity approximations to reduce computational cost [Peherstorfer et al., 2018] while supporting both single and multi-objective optimization. We further introduce layer-wise and depth-wise search spaces for finer-grained merging while also enhancing search efficiency by narrowing the search dimensions. Our key contributions include:

- We propose an automated model merging framework that enhances both single and multi-objective reasoning capabilities while reducing computational costs through multi-level fidelity optimization.
- We introduce two novel search spaces: Layer-wise Fusion Space (LFS) for fine-grained layer merging and Depth-wise Integration Space (DIS) for optimizing inference pathways, enabling comprehensive model integration strategies while reducing search complexity.
- We demonstrated efficient optimization across different scenarios: in mathematical reasoning using LFS, only 17% of trials required the full search budget within 500 trials; in general reasoning using DIS, only 18.6% of trials required the full budget within 1000 trials.
- We achieve significant performance gains, including a 6.86% average improvement in multi-objective scenarios and a 4.24% improvement on the challenging GSM8K task, with consistent effectiveness across various reasoning benchmarks.

2 Related Work

Model Merging Model merging enhances capabilities without additional training data or extensive computation. The field evolved from simple weighted parameter averaging [Utans, 1996] to advanced methods. Task Arithmetic [Ilharco et al., 2022] computes parameter differences, SLERP [White, 2016] implements spherical interpolation, TIES-Merging [Yadav et al., 2024] selectively retains parameters based on magnitude while addressing sign conflicts, DARE [Yu et al., 2024] combines magnitude-based sparsification with parameter rescaling. Recent Evolutionary model merging [Akiba et al., 2024] optimizes coefficients through evolutionary search but is limited by uniform layer merging and excessive search space volume. Our framework introduces a fine-grained search space with reduced dimensionality, leveraging Multi-fidelity optimization [Peherstorfer et al., 2018] for efficient merging recipe optimization.

Hyperparameter Optimization Bayesian Optimization shows success in various applications [Snoek et al., 2012, Mendoza et al., 2016]. Gaussian processes provide strong uncertainty estimates but lack scalability. Alternative models like Random forests [Hutter et al., 2011] and Bayesian neural networks [Snoek et al., 2015] address this limitation by offering better high-dimensional scaling. Hyperband, a multi-fidelity method [Peherstorfer et al., 2018], allocates resources efficiently with successive halving [Jamieson and Talwalkar, 2016], but its random sampling ignores previous evaluations. Our optimizer leverages SMAC [Lindauer et al., 2022], combining Hyperband with Bayesian Optimization for efficient resource allocation and improved learning through surrogate modeling.

3 Motivation

Current merging methods typically incorporate layerwise and depthwise modifications to maintain architectural stability while avoiding costly post-finetuning [Ilharco et al., 2022, White, 2016, Kim et al., 2023]. However, despite their effectiveness, these approaches face inevitable limitations.

Limitations of Current Approaches For layer-wise merging, most methods [Ilharco et al., 2022, White, 2016, Yadav et al., 2024, Yu et al., 2024] focus on combining corresponding layers from multiple models.

While effective, these approaches typically apply uniform merging methods and hyperparameters

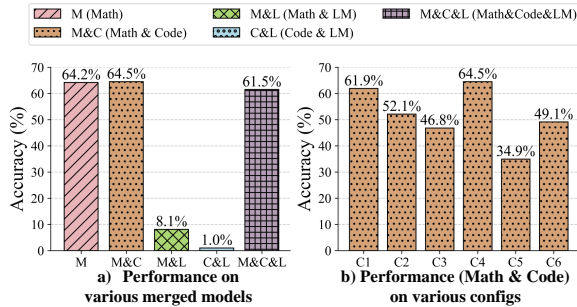


Figure 1: Performance evaluation with TIES on the GSM8K benchmark: (a) comparison of different source model combinations and (b) various configurations with Math and Code as source models.

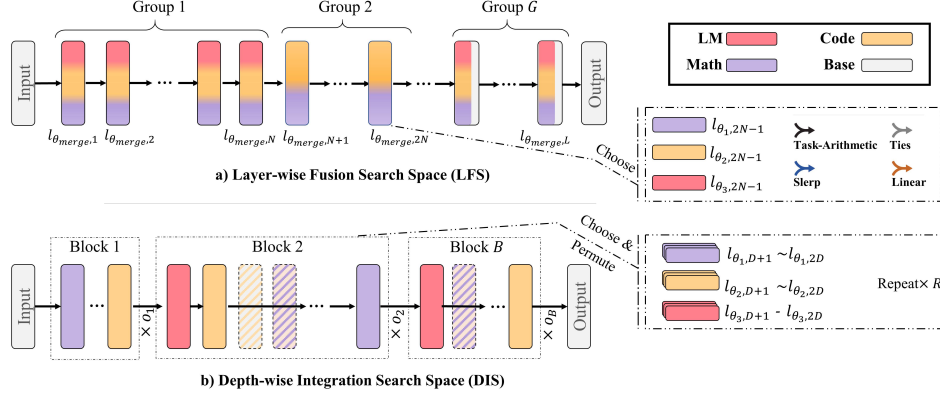


Figure 2: Illustrations of two merging search spaces: (a) Layer-wise Fusion Search (LFS), which merges layers across layer groups with different methods and hyper-parameters, and (b) Depth-wise Integration Search (DIS), which optimizes inference paths through block-wise searching with permutation and layer selection from different source models.

across all layers, using the entire set of candidate models, which might be too coarse-grained and potentially problematic. To illustrate this concern, we conduct an analysis using TIES [Yadav et al., 2024], one of the most robust merging methods, combining WizardLM-13B(LM) [Xu et al., 2023], WizardMath-13B(Math) [Luo et al., 2023a], and llama-2-13b-code-alpaca(Code) [Chaudhary, 2023] on the GSM8K [Cobbe et al., 2021] benchmark. We set the scaling term and parameter retention ratio in reasonable ranges of [0.5, 1.0] and [0.5, 0.7, 0.9], respectively. See Table 7 for detailed configuration information. As shown in Figure 1(a), when applying TIES merge with the same hyper-parameters across different model combinations, the accuracy varies dramatically from 1% to 64.5%. Furthermore, Figure 1(b) demonstrates that even with a fixed model combination (Math+Code), different hyperparameter settings lead to substantial performance variations, ranging from 34.9% to 64.5%. These results reveal two critical challenges in layer-wise merging: the selection of candidate models and the determination of hyperparameters. Both factors significantly impact the final performance, even for well-established methods like TIES. For depth-wise merging approaches, such as Solar [Kim et al., 2023], which simply scales large language models through concatenation of models, the resulting models exhibit insufficient performance and require further expensive pretraining to meet downstream task requirements, which further underscores the critical importance of hyperparameter selection. Manual tuning of these hyperparameters is not only labor-intensive but also makes it challenging to find optimal configurations.

Automatic Model Merging The above concerns highlight that automatic model merging remains largely unexplored. Recent advances include Evolutionary model merging [Akiba et al., 2024], which optimizes merging coefficients through automatic evolutionary search. However, It’s limited by uniform layer merging and exploration of all possible layer interactions, creating an excessively large search space that hinders optimization. We aim to provide a more fine-grained and effective automatic merging framework. A comprehensive comparison with Evolutionary model merging [Akiba et al., 2024] appears in the Appendix C. We present our methods in the following sections.

4 Methods

4.1 Overview

To define a hyperparameter optimization pipeline for model merging, we need three parts, a search space that determines how models are merged by designed configuration, objective functions that evaluate desired capabilities of the merged model, and an efficient search optimizer that identifies optimal configurations. **(1) Search spaces:** We introduce two complementary search spaces. LFS enables fine-grained merging of corresponding layers through optimal merge operations, while DIS addresses models lacking mergeable corresponding layers by optimizing sequential arrangement of preserved layer weights. **(2) Objectives:** Our framework supports both task-specific optimization and Pareto-optimal configurations across multiple reasoning dimensions. **(3) Optimizer:** We implement a multi-fidelity optimizer that accelerates search by efficiently allocating computational resources to promising candidate architectures.

4.2 Search Space

4.2.1 Layer-wise Fusion Search Space

We design a fine-grained layer-wise merging search space (LFS). Our search space is illustrated in Figure 2 (a), we partition the model’s L layers into G consecutive groups, where layers within each group share the same merging coefficients. These coefficients determine: (1) the selection of source models from the candidate pool, (2) the choice of merging algorithms, and (3) the corresponding hyperparameters for the chosen merging method. Inspired by studies showing specialized functions in neural architectures where MLPs store facts [Geva et al., 2020] and attention captures relations between concepts [Wang et al., 2022], we further introduce a component-wise decomposition strategy. Specifically, we partition the parameters within each Transformer layer into C component groups. When $C = 1$, the entire layer is treated as a single unit. When $C = 3$, we decompose the layer into three groups: MLP-related parameters, attention mechanism parameters, and layer normalization parameters. This decomposition facilitates a better way of preserving the unique functional contributions of each architectural element.

We define the merging coefficients $x \in \mathbb{R}^{G \times C \times (1+H)}$, where G represents the number of layer groups, C denotes the number of components per layer, and $1 + H$ dimensions specify the merging method selection and hyperparameters of all candidate merging methods. We use four well-established merging methods: Task Arithmetic, TIES-Merging, SLERP, and Linear Merging. See Section A.2 for additional information. LFS provides a fine-grained and flexible search space for model merging through multiple merging methods, layer selection, and granular controls, which not only enables precise optimization of the fusion but also maximizes the potential of layer-wise merging.

4.2.2 Depth-wise Integration Search Space

Large Language Models (LLMs) exhibit hierarchical language understanding, with knowledge transformation progressing sequentially from word-level comprehension to abstract conceptual understanding. Recent research has increasingly focused on the behavior of transformer layers. Meng et al. [2022] and Geva et al. [2022] explored the distribution of knowledge across different layers. Lad et al. examined the robustness of transformer-based large language models by analyzing the effects of layer deletion and swapping. Sun et al. [2024] show that lower and final layers differ from middle layers, which demonstrate uniformity and robustness to reordering and parallelization for certain tasks. This hierarchical relationship between layers remain unexplored in the context of model merging. To fill this gap, we introduce the Depth-wise Integration Search Space (DIS), which preserves the original weights of individual layers while optimizing the inference pathway.

As depicted in Figure 2 (b), DIS is characterized by three parameters: depth granularity D , number of candidate models M , and repeat factor R . These parameters partition transformer layers into $B = L/D$ consecutive blocks, where each block encompasses $D \times M \times R$ candidate layers. The search space is characterized by merging coefficients $x = \{(\mathbf{s}^{(i)}, \mathbf{p}^{(i)}, o_i)\}_{i=1}^B$, where selection vector $\mathbf{s}^{(i)} \in \{0, 1\}^{M \times D \times R}$ determines layer activation and permutation vector $\mathbf{p}^{(i)} \in \{0, 1, \dots, P-1\}$ with $P = (D \times M \times R)! / (R!)^{M \times D}$ specifies layer ordering, and scaling factor o_i normalizes the output of each block [Akiba et al., 2024]. When no layers are selected in a block ($\mathbf{s}^{(i)} = 0$), we implement a layer retention strategy that preserves model depth by defaulting to base model layers.

The parameterization enables various architectural operations (pruning, stacking, repetition, re-ordering) controlled by granularity parameter D . At $D = 1$, the search space focuses on position-corresponding layer interactions, while increasing D allows more complex integration patterns and cross-depth interactions. This approach controls layer interaction through depth granularity, enabling flexible task adjustment while reducing search space with fewer hyperparameters.

4.3 Objectives

Single objective We use single-objective to maximize task-specific performance. The cost function for each task is defined as $c_i(x) = \arg \min_{x \in \Lambda} \mathcal{L}(\mathcal{D}_i; x)$, where $c_i(x)$ represents an optimization objective over the parameter space x for a specific task dataset \mathcal{D}_i . The loss function \mathcal{L} measures the model’s performance on the target task dataset.

Multi objective To develop comprehensive reasoning models, we employ ParEGO [Knowles, 2006] for multi-objective optimization to identify Pareto-optimal solutions across different objectives. The algorithm converts multiple cost functions into a single aggregated cost using a parameterized scalarizing weight vector. By varying this weight vector at each iteration, ParEGO gradually builds an approximation of the entire Pareto front. Initially, the algorithm normalizes the k cost functions $c_j(x)$ to the $[0, 1]$ interval. In each step, the algorithm randomly selects a weight vector λ from a set of uniformly distributed vectors, defined as:

$$\Lambda = \left\{ \lambda = (\lambda_1, \lambda_2, \dots, \lambda_k) \mid \sum_{j=1}^k \lambda_j = 1 \wedge \forall j, \lambda_j = \frac{l}{s}, l \in \{0, \dots, s\} \right\}$$

The size of this set is determined by $|\Lambda| = \binom{s+k-1}{k-1}$, where s controls the total number of possible vectors. The aggregated cost c_{agg} for each solution x is calculated using the augmented Tchebycheff function, where ρ is a small positive constant that ensures Pareto optimality:

$$c_{\text{agg}}(x; \lambda) = \max_{j=1}^k (\lambda_j \cdot c_j(x)) + \rho \sum_{j=1}^k \lambda_j \cdot c_j(x) \quad (1)$$

4.4 Multi-Fidelity Optimization

Although optimization of model merging requires less computation compared to searching for optimal hyper-parameters for neural network structures and the model training process [Yu and Zhu, 2020, Elsken et al., 2019], evaluating large language models on extensive validation datasets remains computationally intensive. We optimize the process using cost-efficient Multi-Fidelity Optimization (MFO) [Peherstorfer et al., 2018], leveraging evaluations across different fidelity levels from fast but less accurate low-fidelity to slow but more accurate high-fidelity. The optimization objective can be formulated as $x^* \in \arg \min_{x \in \Lambda} c(x, b)$. Here, we use evaluation sample size as fidelity types, represented by budgets b where $b_{\min} \leq b \leq b_{\max}$. Each configuration is evaluated with varying budgets $b_{\min} \leq b \leq b_{\max}$. Using smaller budgets provides a cheaper proxy of the true cost function.

Our implementation extends SMAC [Lindauer et al., 2022] by establishing a hierarchical evaluation framework parameterized by b_{\max} , b_{\min} , and spacing factor η . The number of brackets is determined by $s_{\max} = \lfloor \log_{\eta}(b_{\max}/b_{\min}) \rfloor$, with each bracket s starting with $n_s = \lceil \frac{s_{\max}+1}{s+1} \cdot n \rceil$ configurations at budget $b_s = b_{\min} \cdot \eta^s$. Using Successive Halving [Jamieson and Talwalkar, 2016], each bracket iteratively halves configurations and increases budgets by η until reaching b_{\max} . A Random Forest surrogate model [Breiman, 2001] guides configuration selection through Expected Improvement. Optimization terminates when total budget is exhausted, maximum iterations reached, or performance plateaus. See Section A.3 for more descriptions of the optimization.

5 Experiments

5.1 Experimental Setting

Source Models We use Llama-family models [Touvron et al., 2023] as base model set, including WizardLM-13B(LM) [Xu et al., 2023], WizardMath-13B(MATH) [Luo et al., 2023a], and llama-2-13b-code-alpaca(CODE) [Chaudhary, 2023]. All these models are fine-tuned from Llama-2-13b, ensuring a shared loss landscape. We exclude WizardCoder-Python-13B [Luo et al., 2023b] as it uses a different pre-trained backbone, resulting in a different loss landscape.

Datasets We select separate datasets for search and evaluation. For searching, we use GSMPlus [Li et al., 2024] for mathematical reasoning, MBPP [Austin et al., 2021] samples for code understanding, and MMLU [Hendrycks et al., 2020] validation samples for general knowledge. For evaluation, we employ established benchmark test sets: GSM8K [Cobbe et al., 2021] and MATH [Hendrycks et al., 2021] for mathematical reasoning, MBPP and HumanEval [Chen et al., 2021] for code generation, and the MMLU test set for general knowledge assessment. See Section A.4 and A.5 for more details.

Search Spaces As described in the method section, within LFS we implement four merging methods: Task Arithmetic, TIES-Merging, Linear-merging, and Slerp. We set the number of layer groups to

Table 1: Performance comparison of merged models combining WizardLM-13B (LM), WizardMath-13B (Math), and llama-2-13b-codealpaca (Code). For single-objective optimization, improvements over source models are shown in blue. For multi-objective optimization, improvements over the best base model (Math) are shown in blue in the Average column.

				Common		Math		Code		
Method	Model	Source*	Search*	MMLU	GSM8K	MATH	MBPP	HumanEval	Average	
Base	Math	–	–	52.04	64.22	13.70	18.20	7.32	31.10	
	Code	–	–	52.79	0.00	0.00	27.20	23.17	20.63	
	LM	–	–	53.43	3.79	0.00	33.40	38.41	25.81	
Basic	Ties	M+C+L	–	54.67	61.56	10.58	27.40	23.17	35.48 (+4.38)	
	Task Arith	M+C+L	–	54.85	57.99	12.06	26.22	24.04	35.03 (+3.93)	
	Linear	M+C+L	–	55.13	57.09	9.98	29.80	18.90	34.18 (+3.08)	
Evo-Single-Obj	MATH-LFS-EVO	M+C+L	1	54.46	<u>63.53</u> (-0.69)	10.76	30.80	17.07	–	
	CODE-LFS-EVO	M+C+L	2	54.99	64.29	11.16	<u>31.00</u> (-2.40)	23.17	–	
	GEN-LFS-EVO	M+C+L	3	<u>55.00</u> (+1.57)	51.25	8.58	30.40	25.61	–	
Ours-Single-Obj	MATH-LFS	M+C+L	1	54.52	68.46 (+4.24)	10.42	28.20	17.07	–	
	CODE-LFS	M+C+L	2	53.36	49.73	9.30	33.60 (+0.20)	14.63	–	
	GEN-LFS	M+C+L	3	55.31 (+1.88)	33.81	3.82	30.80	16.46	–	
	GEN-DIS-0	M+C+L	3	<u>54.72</u> (+1.29)	16.98	1.14	12.40	9.76	–	
	GEN-DIS-1	L	3	<u>54.76</u> (+1.33)	1.74	0.06	16.80	18.29	–	
Ours-Multi-Obj	MULTI-LFS-0	M+C+L	1-3	55.03	63.08	11.76	32.60	21.95	36.88 (+5.78)	
	MULTI-LFS-1	M+C+L	1-3	54.70	66.94	11.38	30.60	23.78	37.48 (+6.38)	
	MULTI-LFS-2	M+C+L	1-3	54.67	65.13	11.06	30.40	20.73	36.40 (+5.30)	
	MULTI-LFS-3	M+C+L	1-3	54.99	65.50	9.42	30.20	23.17	36.66 (+5.56)	
	MULTI-LFS-4	M+C+L	1-3	54.77	66.79	12.06	31.80	24.40	37.96 (+6.86)	

*Dataset Index: 1=GSMPlus, 2=MBPP_{val}, 3=MMLU_{val}

*M+C+L = Math+Code+LM

$G = 4$ and the number of component groups per layer to $C = 3$. For DIS, we evaluate two configurations: Configuration 1 with depth granularity $D = 1$, number of candidate models $M = 3$, and repeat factor $R = 1$; Configuration 2 with $D = 1$, $M = 1$, and $R = 2$. Both configurations keep $D = 1$ because reasoning tasks exhibit sensitivity to layer ordering, where variations can degrade performance Sun et al. [2024], constraining broader exploration. We focus on layer-wise interactions between corresponding positions across candidate models. The two configurations were designed to be complementary: Configuration 1 targets interactions across models, whereas Configuration 2 targets repeated layers within a model. We set a maximum layer constraint of 50 to manage computational costs.

Objectives and Optimization We define task-specific single objectives using accuracy performance on specialized datasets: GSMPlus [Li et al., 2024] for mathematical reasoning, MBPP [Austin et al., 2021] validation set for programming capabilities, and MMLU [Hendrycks et al., 2020] validation set for general reasoning. For multi-objective optimization, we seek Pareto-optimal solutions across these three tasks. Our optimizer builds upon SMAC [Lindauer et al., 2022], with domain-specific budget allocations for optimization tasks. Mathematical reasoning tasks receive 100-1000 samples to explore complex solution spaces, code reasoning uses 300 samples (200 training, 100 validation), and we sample 50% of MMLU validation data within 100-700 sample bounds for general reasoning. These budget ranges remain consistent when conducting multi-objective optimization across multiple datasets within these domains. We configured the search trials based on the complexity of each search space. We allocated 500 search trials for LFS and 1000 for the broader DIS search space, using initial candidate models as starting points to improve optimization efficiency.

5.2 Results

5.2.1 Single objective optimization

Layer-wise Fusion Using three source models (Math, Code, and LM) optimized for mathematical, coding, and general reasoning tasks respectively, we developed three specialized models through LFS: MATH-LFS, CODE-LFS, and GEN-LFS. Table 1 presents the performance of these models across five benchmarks. Our results demonstrate that MATH-LFS achieves a 4.24% improvement over the best performance of source models on GSM8K, CODE-LFS shows modest gains on MBPP, and GEN-LFS exhibits a 1.88% improvement on MMLU. These MATH-LFS gains are especially surprising, given that the base model was already finetuned for improve GSM8K performance - it

Table 2: Performance of models merged via LFS and DIS on other Reasoning Tasks. LFS+DIS represents using LFS-merged model as an additional source model for DIS search. Numbers in blue indicate improvements over the best source model.

Benchmark	Source Models				Merging Results		
	Math	Code	LM	LM_JA	LFS	DIS	LFS+DIS
LogiQA	29.65	25.81	28.57	–	30.88 (+1.23)	29.34 (-0.31)	31.64 (+1.99)
OpenBookQA	34.20	34.80	34.40	–	37.60 (+2.80)	37.40 (+2.60)	38.60 (+3.80)
OpenBookQA+f	39.20	44.20	46.20	–	47.00 (+0.80)	47.40 (+1.20)	47.80 (+1.60)
PIQA	79.77	79.92	79.95	–	80.93 (+0.98)	79.02 (-0.93)	80.03 (+0.08)
SocialQA	46.82	46.77	51.09	–	51.14 (+0.05)	50.50 (-0.59)	50.17 (-0.92)
MGSM_JA	8.00	4.00	10.40	–	17.60 (+7.20)	15.20 (+4.80)	22.00 (+10.60)
MGSM_JA	8.00	–	–	8.80	16.40 (+7.60)	21.60 (+12.80)	19.60 (+10.80)

^{*}LM_JA denotes ELYZA-japanese-Llama-2-13b

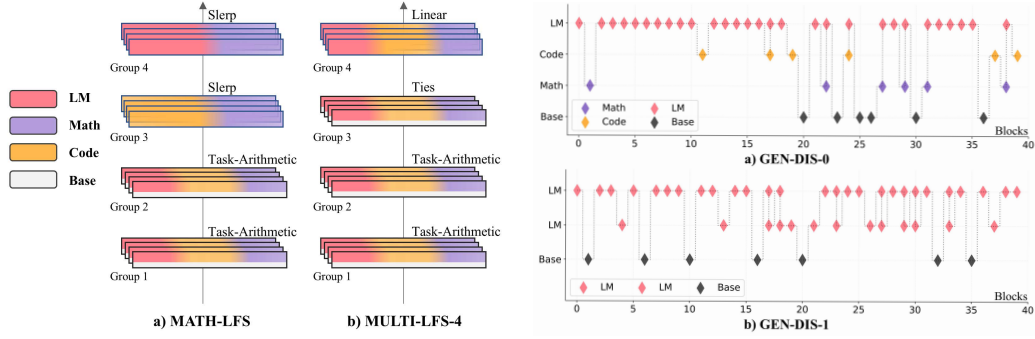
appears that its arithmetic performance could be further improved through merging with the coding and instruction tuning model.

Beyond these task-specific enhancements, we observe that LFS-searched models also demonstrate improved performance in other reasoning capabilities, with MATH-LFS showing particular strength in both common reasoning and code generation tasks, while although both GSM8K and MATH are mathematical tasks, they differ in complexity and scenarios. The merging process appears to overemphasize arithmetic, which is less relevant for MATH, leading to the observed performance drop. In comparison with alternative merging methods including TIES, Task Arithmetic, and linear merging (with hyperparameter search ranges detailed in Table 8), our LFS method achieves superior performance on the targeted optimization objectives, demonstrating the effectiveness of our approach in single task optimization. The architecture of MATH-LFS, as illustrated in Figure 2(a), divides the model layers into four groups (G=4), where Task Arithmetic merge is employed for groups 1 and 2, while the subsequent layer groups 3 and 4 utilize SLERP merge with different model combinations - Math-Code and Math-LM respectively. The full architecture parameters can be found in Table 13. Notably, we found that HumanEval [Chen et al., 2021] is very sensitive to parameter changes. When merging the LM with other models, performance dropped for all methods. This may be due to the nature of the task and the small test set of only 164 samples.

Depth-wise Integration We evaluated two DIS search configurations: Configuration 1 using three candidate models (Code, Math, and LM) with depth granularity 1 and repeat factor 1; and Configuration 2 using a single candidate model (the corresponding source model for specific objective) with depth granularity 1 and repeat factor 2. Using these configurations, we similarly optimized for mathematical, coding, and general reasoning tasks respectively. DIS demonstrated effectiveness only in general reasoning tasks, yielding GEN-DIS-0 and GEN-DIS-1. Our results, as presented in Table 1, demonstrate that both models achieved improvements, exceeding 1% over the source models on the MMLU benchmark. GEN-DIS-0 exhibited enhanced performance not only on the optimization objective but also demonstrated benefits on auxiliary tasks, showing improvement on the GSM8K. A detailed breakdown of performance across MMLU categories is presented in Table 9.

We visualize the network in Figure 2(b). The complete set of architectural parameters can be found in Table 14. GEN-DIS-0 exhibited a predominantly stable selection of LM layers in early layers, gradually incorporating other source model layers with stacking behavior in middle and later layers. Similarly, GEN-DIS-1 demonstrated no layer repetition in early layers but showed emergence of layer repetition patterns after layer 15. Notably, although improvements were observed in common reasoning task, we found no superior configurations for mathematical and code reasoning tasks, suggesting varying sensitivity to layer ordering across different tasks. To further explore our methodology, we extend our investigation to additional tasks.

Expanding to other tasks We further evaluated our method on diverse reasoning tasks including LogicQA [Liu et al., 2020], OpenBookQA [Mihaylov et al., 2018], PIQA [Bisk et al., 2020], SocialQA [Sap et al., 2019], and MGSM Japanese [Sap et al., 2019], using validation datasets for searching and test sets for evaluation. For OpenBookQA, we tested with and without relevant facts in the prompt. We incorporated ELYZA-japanese-Llama-2-13b [Sasaki et al., 2023] alongside our base models (LM, Math, Code) for MGSM Japanese tasks. See Section A.8 for implementation details. Results are presented in Table 2. For most tasks, LFS+DFS shows promising results with significant improvements across benchmarks, notably 3.80% on OpenBookQA and up to 10.8 points on MGSM_JA. In addition to LFS that consistently delivers positive improvements, DFS shows



(a): Visualization of LFS-searched neural architectures: (a) MATH-LFS optimized for arithmetic ability; (b) MULTI-LFS-4 optimized for multiple objectives.

(b): Visualization of DIS model architecture. The x-axis represents block indices from 1 to 40, and the y-axis indicates the selected layer in each block.

occasional degradation in LogiQA and PIQA. The results particularly highlight the effectiveness of our method in cross-lingual reasoning tasks, DIS demonstrates notable effectiveness with improvements up to 12.80 points, We hypothesize DIS’s preservation of processing blocks may be more effective when merging models from complementary domains. The architectural parameters can be found in Tables 15 and 16.

Comparison with Evolutionary-based Searching. For a fair comparison, we conducted controlled experiments within our Layer-wise Fusion Search Space (LFS), evaluating our optimizer against Covariance matrix adaptation evolution strategy (CMA-ES)[Hansen, 2006], as used in [Akiba et al., 2024]. We implemented CMA-ES with a 200-trial budget, matching our search budget (approximately 161 full-budget trials in MATH-LFS, see Table 3). We optimized for mathematical, coding, and general reasoning tasks, respectively, yielding MATH-LFS-EVO, CODE-LFS-EVO, and GEN-LFS-EVO models, which we compared against our MATH-LFS, CODE-LFS, and GEN-LFS models. As shown in Table 1, our approach consistently outperformed the evolutionary method across all tasks, demonstrating that our multi-fidelity optimizer enables more effective search space exploration.

5.2.2 Multi objective Optimization

Given the task-specific nature of DIS search and the more robust merging capabilities of LFS, we conducted our multi objective search on LFS with three optimization objectives: mathematical reasoning, code generation, and general reasoning. Our optimization yielded five Pareto-optimal solutions, denoted as MULTI-LFS-0 to MULTI-LFS-4, with their performance metrics presented in Table 1. These solutions achieved significant improvements, ranging from 5.30 to 6.86 points on average compared to the best candidate model. When comparing our results with existing merging approaches such as Ties, task arithmetic, and linear merging, our method achieves better trade-offs along the Pareto frontier while maintaining higher average performance across all benchmarks. This demonstrates the inherent multi-task nature of large models and effectiveness of our multi-objective optimization strategy in finding superior model configurations that balance diverse task requirements.

As visualized in Figure 2(a), our analysis of MULTI-LFS-4 reveals an interesting layer-wise merging pattern: Task Arithmetic is optimal for groups 1 and 2, while groups 3 and 4 employ Ties and linear merging strategies. Unlike the single-objective search-derived MATH-LFS, MULTI-LFS-4 shows a preference for incorporating layers from all source models during the merging process, resulting in better preservation of comprehensive information. Experiments with fixed merging methods (only TIES or Task Arithmetic) show performance drops, with details in table 10.

Table 3: Statistics of searching trials across budget levels for MATH-LFS and GEN-DIS-1.

	MATH-LFS			GEN-DIS-1			
	100	300	1000	0	100	300	700
Trail Count	263	152	85	196	311	307	186
Percentage (%)	52.6	30.4	17.0	19.6	31.1	30.7	18.6

Table 4: Ablation study on granularity (G) and component groups (C) for MATH-LFS search.

Component Groups	Layer Groups (G)			
	10	4	2	1
$C=3$	66.79	68.46	67.82	66.41
$C=1$	66.41	68.08	67.24	66.41

5.2.3 Efficiency Analysis

Our Multi-Fidelity Optimizer dynamically adjusts budget allocation during search, with budget defined as validation dataset size. Here, we analyze the budget distribution during the search process using MATH-LFS and GEN-DIS-1 as examples (see Table 11 for complete details). As shown in Table 3, For MATH-LFS(500 trials with budgets of 100, 300, and 1000), Only 17% of trials used the full budget, while 52% used the minimum budget. For GEN-DIS-1, we set a maximum layer constraint of 50 to manage computational costs, with configurations exceeding this receiving zero budget. Of 1000 initial trials, 804 were effective, with only 18.6% using full evaluation budget. This approach significantly reduced computational costs while maintaining solution quality.

6 Ablations and Analysis

Impact of granularity in LFS. To examine the effect of granularity in layer-wise fusion search space, we conducted ablation studies to examine the effect of granularity in LFS by varying the number of layer groups (G) and component groups (C). Table 4 shows that increasing G from 1 to 4 consistently improves GSM8K accuracy, demonstrating the benefits of more fine-grained layer control. However, performance decreases when G reaches 10, likely due to the growth in search space exceeding our search algorithm’s capability within the given trials. Our analysis also shows that increasing C from 1 to 3 improves performance, though these gains are smaller compared to layer-wise refinement.

Table 5: Ablation study on layer retention for GEN-DIS-1 model. GEN-DIS-1-NR denotes GEN-DIS-1 without layer retention.

Model	Benchmarks					Source Models			SFS Results		
	MMLU	GSM8K	MATH	MBPP	HumanEval	Math	Code	LM	SFS-0	SFS-1	SFS-2
LM	53.43	3.79	0.00	33.40	38.41	52.04	52.79	53.43	52.03	51.91	53.63 ↑
GEN-DIS-1	54.76 ↑	1.74	0.06	16.80	18.29	64.22	0.00	3.79	63.91 ↓	0.00	6.52
GEN-DIS-NR	53.68 ↑	1.82	0.02	9.80	4.88	13.70	0.00	0.00	13.58	0.00	0.08
						18.20	27.20	33.40	18.20	28.60 ↑	30.40
						7.32	23.17	38.41	7.32	24.39	34.15

Impact of layer retention in DIS. To explore the layer retention strategy in our DIS search space, we conducted a comparative experiment. Specifically, we modified the DIS-GEN-1 configuration by replacing the layer retention strategy with direct layer deletion, resulting in the DIS-GEN-NR. As shown in Table 5, although it marginally outperformed the baseline language model on MMLU, its performance still fell short compared to our proposed layer retention approach. This result shows that directly deleting layers degrades model performance while retaining layers is more effective.

Search only for rescaling. Several findings show that finetuning [Zhang et al., 2024] or scaling [Christ et al., 2024] task-specific neurons can improve model performance. To evaluate these claims and to verify that our DIS search space (which includes scales) is not simply rescaling layers, we further evaluate Scale-Factor Search Space (SFS) that optimizes tasks by searching scaling factors to weights and layer outputs. As before, we apply our framework and obtain three SFS models: SFS-MATH, SFS-CODE, and SFS-GEN, each initialized from specialized base models. As shown in Table 6, results show a decline in mathematical performance and slight improvements in code and reasoning tasks, though gains are modest compared to LFS and DIS, showing that scale optimization alone is not sufficient to explain the DIS effectiveness.

7 Conclusions and Future Work

We presented a multi-fidelity framework for automated model merging with two complementary search spaces: Layer-wise Fusion Search for fine-grained layer merging and Depth-wise Integration Search for optimizing sequential layer arrangements. We show automated model merging not only works, but is quite effective, demonstrating strong performance in both single-objective and multi-objective scenarios, achieving a 4.24% improvement on the GSM8K challenge task with only 17% of the full budget within 500 trials, and a 6.86% improvement in multi-objective performance using 18.6% of the full budget within 1000 trials. When extended to various benchmarks, our method consistently shows promising results without any additional tuning. Overall, our work provides an efficient and flexible framework for automated model merging that achieves effective improvements with reduced computational costs. However, merged models may inherit biases from source models, requiring thorough evaluation before deployment.

References

- Takuya Akiba, Makoto Shing, Yujin Tang, Qi Sun, and David Ha. Evolutionary optimization of model merging recipes. *arXiv preprint arXiv:2403.13187*, 2024.
- Jacob Austin, Augustus Odena, Maxwell Nye, Maarten Bosma, Henryk Michalewski, David Dohan, Ellen Jiang, Carrie Cai, Michael Terry, Quoc Le, et al. Program synthesis with large language models. *arXiv preprint arXiv:2108.07732*, 2021.
- Xiao Bi, Deli Chen, Guanting Chen, Shanhuang Chen, Damai Dai, Chengqi Deng, Honghui Ding, Kai Dong, Qiusi Du, Zhe Fu, et al. Deepseek llm: Scaling open-source language models with longtermism. *arXiv preprint arXiv:2401.02954*, 2024.
- Yonatan Bisk, Rowan Zellers, Jianfeng Gao, Yejin Choi, et al. Piqa: Reasoning about physical commonsense in natural language. In *Proceedings of the AAAI conference on artificial intelligence*, volume 34, pages 7432–7439, 2020.
- Leo Breiman. Random forests. *Machine learning*, 45:5–32, 2001.
- Sahil Chaudhary. Code alpaca: An instruction-following llama model for code generation. *GitHub repository*, 2023.
- Mark Chen, Jerry Tworek, Heewoo Jun, Qiming Yuan, Henrique Ponde de Oliveira Pinto, Jared Kaplan, Harri Edwards, Yuri Burda, Nicholas Joseph, Greg Brockman, Alex Ray, Raul Puri, Gretchen Krueger, Michael Petrov, Heidy Khlaaf, Girish Sastry, Pamela Mishkin, Brooke Chan, Scott Gray, Nick Ryder, Mikhail Pavlov, Alethea Power, Lukasz Kaiser, Mohammad Bavarian, Clemens Winter, Philippe Tillet, Felipe Petroski Such, Dave Cummings, Matthias Plappert, Fotios Chantzis, Elizabeth Barnes, Ariel Herbert-Voss, William Hebgen Guss, Alex Nichol, Alex Paino, Nikolas Tezak, Jie Tang, Igor Babuschkin, Suchir Balaji, Shantanu Jain, William Saunders, Christopher Hesse, Andrew N. Carr, Jan Leike, Josh Achiam, Vedant Misra, Evan Morikawa, Alec Radford, Matthew Knight, Miles Brundage, Mira Murati, Katie Mayer, Peter Welinder, Bob McGrew, Dario Amodei, Sam McCandlish, Ilya Sutskever, and Wojciech Zaremba. Evaluating large language models trained on code. 2021.
- Bryan R Christ, Zack Gottesman, Jonathan Kropko, and Thomas Hartvigsen. Math neurosurgery: Isolating language models’ math reasoning abilities using only forward passes. *arXiv preprint arXiv:2410.16930*, 2024.
- Karl Cobbe, Vineet Kosaraju, Mohammad Bavarian, Mark Chen, Heewoo Jun, Lukasz Kaiser, Matthias Plappert, Jerry Tworek, Jacob Hilton, Reiichiro Nakano, et al. Training verifiers to solve math word problems. *arXiv preprint arXiv:2110.14168*, 2021.
- Thomas Elsken, Jan Hendrik Metzen, and Frank Hutter. Neural architecture search: A survey. *Journal of Machine Learning Research*, 20(55):1–21, 2019.
- Leo Gao, Jonathan Tow, Baber Abbasi, Stella Biderman, Sid Black, Anthony DiPofi, Charles Foster, Laurence Golding, Jeffrey Hsu, Alain Le Noac’h, Haonan Li, Kyle McDonell, Niklas Muennighoff, Chris Ociepa, Jason Phang, Laria Reynolds, Hailey Schoelkopf, Aviya Skowron, Lintang Sutawika, Eric Tang, Anish Thite, Ben Wang, Kevin Wang, and Andy Zou. A framework for few-shot language model evaluation, 07 2024. URL <https://zenodo.org/records/12608602>.
- Mor Geva, Roei Schuster, Jonathan Berant, and Omer Levy. Transformer feed-forward layers are key-value memories. *arXiv preprint arXiv:2012.14913*, 2020.
- Mor Geva, Avi Caciularu, Kevin Ro Wang, and Yoav Goldberg. Transformer feed-forward layers build predictions by promoting concepts in the vocabulary space. *arXiv preprint arXiv:2203.14680*, 2022.
- Daya Guo, Qihao Zhu, Dejian Yang, Zhenda Xie, Kai Dong, Wentao Zhang, Guanting Chen, Xiao Bi, Yu Wu, YK Li, et al. Deepseek-coder: When the large language model meets programming—the rise of code intelligence. *arXiv preprint arXiv:2401.14196*, 2024.
- Nikolaus Hansen. The cma evolution strategy: a comparing review. *Towards a new evolutionary computation: Advances in the estimation of distribution algorithms*, pages 75–102, 2006.

- Dan Hendrycks, Collin Burns, Steven Basart, Andy Zou, Mantas Mazeika, Dawn Song, and Jacob Steinhardt. Measuring massive multitask language understanding. *arXiv preprint arXiv:2009.03300*, 2020.
- Dan Hendrycks, Collin Burns, Saurav Kadavath, Akul Arora, Steven Basart, Eric Tang, Dawn Song, and Jacob Steinhardt. Measuring mathematical problem solving with the math dataset. *NeurIPS*, 2021.
- Frank Hutter, Holger H Hoos, and Kevin Leyton-Brown. Sequential model-based optimization for general algorithm configuration. In *Learning and Intelligent Optimization: 5th International Conference, LION 5, Rome, Italy, January 17-21, 2011. Selected Papers 5*, pages 507–523. Springer, 2011.
- Gabriel Ilharco, Marco Tulio Ribeiro, Mitchell Wortsman, Suchin Gururangan, Ludwig Schmidt, Hannaneh Hajishirzi, and Ali Farhadi. Editing models with task arithmetic. *arXiv preprint arXiv:2212.04089*, 2022.
- Kevin Jamieson and Ameet Talwalkar. Non-stochastic best arm identification and hyperparameter optimization. In *Artificial intelligence and statistics*, pages 240–248. PMLR, 2016.
- Albert Q Jiang, Alexandre Sablayrolles, Arthur Mensch, Chris Bamford, Devendra Singh Chaplot, Diego de las Casas, Florian Bressand, Gianna Lengyel, Guillaume Lample, Lucile Saulnier, et al. Mistral 7b. *arXiv preprint arXiv:2310.06825*, 2023.
- Dahyun Kim, Chanjun Park, Sanghoon Kim, Wonsung Lee, Wonho Song, Yunsu Kim, Hyeonwoo Kim, Yungi Kim, Hyeonju Lee, Jihoo Kim, et al. Solar 10.7 b: Scaling large language models with simple yet effective depth up-scaling. *arXiv preprint arXiv:2312.15166*, 2023.
- Joshua Knowles. Parego: A hybrid algorithm with on-line landscape approximation for expensive multiobjective optimization problems. *IEEE transactions on evolutionary computation*, 10(1): 50–66, 2006.
- Woosuk Kwon, Zhuohan Li, Siyuan Zhuang, Ying Sheng, Lianmin Zheng, Cody Hao Yu, Joseph E. Gonzalez, Hao Zhang, and Ion Stoica. Efficient memory management for large language model serving with pagedattention. In *Proceedings of the ACM SIGOPS 29th Symposium on Operating Systems Principles*, 2023.
- Vedang Lad, Wes Gurnee, and Max Tegmark. The remarkable robustness of llms: Stages of inference?, 2024. URL <https://arxiv.org/abs/2406.19384>.
- Lisha Li, Kevin Jamieson, Giulia DeSalvo, Afshin Rostamizadeh, and Ameet Talwalkar. Hyperband: A novel bandit-based approach to hyperparameter optimization. *Journal of Machine Learning Research*, 18(185):1–52, 2018.
- Qintong Li, Leyang Cui, Xueliang Zhao, Lingpeng Kong, and Wei Bi. Gsm-plus: A comprehensive benchmark for evaluating the robustness of llms as mathematical problem solvers. *arXiv preprint arXiv:2402.19255*, 2024.
- Marius Lindauer, Katharina Eggensperger, Matthias Feurer, André Biedenkapp, Difan Deng, Carolin Benjamins, Tim Ruhkopf, René Sass, and Frank Hutter. Smac3: A versatile bayesian optimization package for hyperparameter optimization. *Journal of Machine Learning Research*, 23(54):1–9, 2022. URL <http://jmlr.org/papers/v23/21-0888.html>.
- Jian Liu, Leyang Cui, Hanmeng Liu, Dandan Huang, Yile Wang, and Yue Zhang. Logiqa: A challenge dataset for machine reading comprehension with logical reasoning. *arXiv preprint arXiv:2007.08124*, 2020.
- Haipeng Luo, Qingfeng Sun, Can Xu, Pu Zhao, Jianguang Lou, Chongyang Tao, Xiubo Geng, Qingwei Lin, Shifeng Chen, and Dongmei Zhang. Wizardmath: Empowering mathematical reasoning for large language models via reinforced evol-instruct. *arXiv preprint arXiv:2308.09583*, 2023a.

- Ziyang Luo, Can Xu, Pu Zhao, Qingfeng Sun, Xiubo Geng, Wenxiang Hu, Chongyang Tao, Jing Ma, Qingwei Lin, and Daxin Jiang. Wizardcoder: Empowering code large language models with evol-instruct. *arXiv preprint arXiv:2306.08568*, 2023b.
- Hector Mendoza, Aaron Klein, Matthias Feurer, Jost Tobias Springenberg, and Frank Hutter. Towards automatically-tuned neural networks. In *Workshop on automatic machine learning*, pages 58–65. PMLR, 2016.
- Kevin Meng, David Bau, Alex Andonian, and Yonatan Belinkov. Locating and editing factual associations in gpt. *Advances in Neural Information Processing Systems*, 35:17359–17372, 2022.
- Todor Mihaylov, Peter Clark, Tushar Khot, and Ashish Sabharwal. Can a suit of armor conduct electricity? a new dataset for open book question answering. *arXiv preprint arXiv:1809.02789*, 2018.
- OpenAI, Josh Achiam, Steven Adler, Sandhini Agarwal, Lama Ahmad, Ilge Akkaya, Florencia Leoni Aleman, Diogo Almeida, Janko Altschmidt, Sam Altman, Shyamal Anadkat, et al. Gpt-4 technical report. *arXiv preprint arXiv:2303.08774*, 2023.
- Benjamin Peherstorfer, Karen Willcox, and Max Gunzburger. Survey of multifidelity methods in uncertainty propagation, inference, and optimization. *Siam Review*, 60(3):550–591, 2018.
- Aditya Ramesh, Mikhail Pavlov, Gabriel Goh, Scott Gray, Chelsea Voss, Alec Radford, Mark Chen, and Ilya Sutskever. Zero-shot text-to-image generation. In *International conference on machine learning*, pages 8821–8831. Pmlr, 2021.
- Chitwan Saharia, William Chan, Saurabh Saxena, Lala Li, Jay Whang, Emily L Denton, Kamyar Ghasemipour, Raphael Gontijo Lopes, Burcu Karagol Ayan, Tim Salimans, et al. Photorealistic text-to-image diffusion models with deep language understanding. *Advances in neural information processing systems*, 35:36479–36494, 2022.
- Maarten Sap, Hannah Rashkin, Derek Chen, Ronan LeBras, and Yejin Choi. Socialliqa: Commonsense reasoning about social interactions. *arXiv preprint arXiv:1904.09728*, 2019.
- Akira Sasaki, Masato Hirakawa, Shintaro Horie, Tomoaki Nakamura, Sam Passaglia, and Daisuke Oba. Elyza-japanese-llama-2-13b, 2023. URL <https://huggingface.co/elyza/ELYZA-japanese-Llama-2-13b>.
- Jasper Snoek, Hugo Larochelle, and Ryan P Adams. Practical bayesian optimization of machine learning algorithms. *Advances in neural information processing systems*, 25, 2012.
- Jasper Snoek, Oren Rippel, Kevin Swersky, Ryan Kiros, Nadathur Satish, Narayanan Sundaram, Mostofa Patwary, Mr Prabhat, and Ryan Adams. Scalable bayesian optimization using deep neural networks. In *International conference on machine learning*, pages 2171–2180. PMLR, 2015.
- Qi Sun, Marc Pickett, Aakash Kumar Nain, and Llion Jones. Transformer layers as painters. *arXiv preprint arXiv:2407.09298*, 2024.
- Hugo Touvron, Thibaut Lavril, Gautier Izacard, Xavier Martinet, Marie-Anne Lachaux, Timothée Lacroix, Baptiste Rozière, Naman Goyal, Eric Hambro, Faisal Azhar, et al. Llama: Open and efficient foundation language models. *arXiv preprint arXiv:2302.13971*, 2023.
- Joachim Utans. Weight averaging for neural networks and local resampling schemes. In *Proc. AAAI-96 Workshop on Integrating Multiple Learned Models*. AAAI Press, pages 133–138. Citeseer, 1996.
- Kevin Wang, Alexandre Variengien, Arthur Conmy, Buck Shlegeris, and Jacob Steinhardt. Interpretability in the wild: a circuit for indirect object identification in gpt-2 small, 2022. URL <https://arxiv.org/abs/2211.00593>, 2, 2022.
- Tom White. Sampling generative networks. *arXiv preprint arXiv:1609.04468*, 2016.
- Can Xu, Qingfeng Sun, Kai Zheng, Xiubo Geng, Pu Zhao, Jiazhan Feng, Chongyang Tao, and Daxin Jiang. Wizardlm: Empowering large language models to follow complex instructions. *arXiv preprint arXiv:2304.12244*, 2023.

Prateek Yadav, Derek Tam, Leshem Choshen, Colin A Raffel, and Mohit Bansal. Ties-merging: Resolving interference when merging models. *Advances in Neural Information Processing Systems*, 36, 2024.

Le Yu, Bowen Yu, Haiyang Yu, Fei Huang, and Yongbin Li. Language models are super mario: Absorbing abilities from homologous models as a free lunch. In *Forty-first International Conference on Machine Learning*, 2024.

Tong Yu and Hong Zhu. Hyper-parameter optimization: A review of algorithms and applications. *arXiv preprint arXiv:2003.05689*, 2020.

Wei Zhang, Chaoqun Wan, Yonggang Zhang, Yiu-ming Cheung, Xinmei Tian, Xu Shen, and Jieping Ye. Interpreting and improving large language models in arithmetic calculation. *arXiv preprint arXiv:2409.01659*, 2024.

Qihao Zhu, Daya Guo, Zhihong Shao, Dejian Yang, Peiyi Wang, Runxin Xu, Y Wu, Yukun Li, Huazuo Gao, Shirong Ma, et al. Deepseek-coder-v2: Breaking the barrier of closed-source models in code intelligence. *arXiv preprint arXiv:2406.11931*, 2024.

A Detailed Experimental Settings

A.1 Details of TIES Configuration for Math and Code Model Merging on GSM8K

Table 7: Performance Comparison with Different Parameters of Ties Merging Method

Parameters	Configuration					
Ratio to retain parameters	0.7	0.5	0.7	0.5	0.9	0.9
Scaling Coefficient	1.0	0.5	0.5	1.0	0.5	1.0
Performance on GSM8k	61.94	52.08	46.78	64.52	34.87	49.05

A.2 Descriptions of Existing Model Merging Methods in Layer-wise Fusion Search Space

Task Arithmetic enhance model capabilities through vector operations by leveraging weighted combinations of task-specific knowledge. Given a base model with weights θ_{pre} and task-specific fine-tuned weights $\{\theta_t^{\text{ft}}\}_{t=1}^n$, task vectors are defined as:

$$\tau_t = \theta_t^{\text{ft}} - \theta_{\text{pre}} \quad (2)$$

The merged weights are then computed through:

$$\theta_{\text{Merge}} = \theta_{\text{pre}} + \lambda \sum_{t=1}^n \tau_t \quad (3)$$

where λ controls the magnitude of task-specific adaptations.

TIES-Merging is a parameter conflict resolution approach that operates in three stages. First, select the top $k\%$ parameters by magnitude of each task vector τ_t :

$$\hat{\tau}_t = \text{TopK}(\tau_t, k) \quad (4)$$

Next, Generating a consensus sign vector by examining the aggregate direction of parameter changes across all tasks:

$$\hat{\gamma} = \text{sgn} \left(\sum_{t=1}^n \hat{\tau}_t \right) \quad (5)$$

Finally, computing the average update magnitude considering only those task vectors whose signs align with the consensus direction:

$$\tilde{\tau} = \text{Average}(\{\hat{\tau}_t : \text{sgn}(\hat{\tau}_t) = \hat{\gamma}\}) \quad (6)$$

The final merged model weights are then computed as:

$$\theta_{\text{Merge}} = \theta_{\text{pre}} + \lambda * \tilde{\tau} \quad (7)$$

SLERP (Spherical Linear Interpolation) computes optimal geodesic paths between model weights through:

$$\text{SLERP}(\theta_1, \theta_2, t) = \frac{\sin((1-t)\omega)}{\sin(\omega)}\theta_1 + \frac{\sin(t\omega)}{\sin(\omega)}\theta_2 \quad (8)$$

where $\omega = \arccos\left(\frac{\langle \theta_1, \theta_2 \rangle}{\|\theta_1\| \|\theta_2\|}\right)$ and $t \in [0, 1]$ is the interpolation parameter.

Linear Merging implements straightforward weighted averaging:

$$\theta_{\text{Linear}} = \sum_{t=1}^n w_t \theta_t \quad (9)$$

where $\sum_{t=1}^n w_t = 1$ and $w_t \geq 0$.

A.3 Descriptions of SMAC-based Multi-Fidelity Optimization

Our implementation extends SMAC [Lindauer et al., 2022], integrating Hyperband (HB) [Li et al., 2018] with Bayesian Optimization (BO) [Snoek et al., 2012] and employing Random Forest [Breiman, 2001] as the surrogate model.

The framework operates using minimum and maximum budgets (b_{\min}, b_{\max}) with a spacing parameter $\eta > 1$. The algorithm creates $s_{\max} = \lfloor \log_{\eta}(b_{\max}/b_{\min}) \rfloor$ brackets, each initiating with $n_i = \lfloor \eta^{s_{\max}-i} \cdot \frac{\eta}{\eta-1} \rfloor$ configurations. Within each bracket, Successive Halving proceeds through $\lfloor \log_{\eta}(\frac{n_i}{n_{\min}}) \rfloor + 1$ rounds, evaluating configurations at increasing budgets while progressively eliminating underperforming candidates. Specifically, after evaluating all configurations at budget b , only the top $\lfloor \frac{n_i}{\eta} \rfloor$ performers advance to the next round with an increased budget of ηb .

A key enhancement is the Random Forest model that learns from all prior configuration-performance pairs, prioritizing data from higher budgets. This model guides the selection of promising configurations via Expected Improvement, balancing exploration and exploitation. As the optimization progresses, the evaluation of more configurations at higher budgets enables the algorithm to correct potential misjudgments from lower-fidelity evaluations.

For a detailed algorithmic description, see Algorithm 1, which presents the complete optimization process incorporating trial limits. This integration of multi-fidelity resource allocation with surrogate-based modeling delivers efficient configuration space exploration while maintaining evaluation quality.

A.4 Details of Datasets Information

For searching, We use data from three reasoning domains: 1,000 GSMPlus [Li et al., 2024] samples, an adversarial variant of GSM8K with mathematical perturbations for testing math reasoning; 300 MBPP [Austin et al., 2021] samples (200 training/100 validation) for code understanding; and 700 samples from MMLU validation [Hendrycks et al., 2020] for general reasoning. These datasets support both single-objective optimization when used separately and multi-objective optimization when combined. For comprehensive performance evaluation, we employ established benchmark test sets across three key domains: mathematical reasoning using the complete test sets from GSM8K [Cobbe et al., 2021] and MATH [Hendrycks et al., 2021], code generation using the standard test splits from MBPP [Austin et al., 2021] and HumanEval [Chen et al., 2021], and general knowledge using the MMLU test set [Hendrycks et al., 2020], which spans diverse knowledge domains.

Algorithm 1 SMAC-based Multi-Fidelity Optimization

Require: Configuration space Θ , minimum budget b_{\min} , maximum budget b_{\max} , spacing factor $\eta > 1$, maximum trials T_{\max}

Ensure: Optimized configuration θ^*

```
1:  $s_{\max} \leftarrow \lfloor \log_{\eta}(\frac{b_{\max}}{b_{\min}}) \rfloor$  ▷ Maximum brackets
2:  $\mathcal{D} \leftarrow \emptyset$  ▷ Observation history
3:  $\theta^* \leftarrow \emptyset, y^* \leftarrow \infty$  ▷ Best configuration tracking
4:  $T \leftarrow 0$  ▷ Initialize trial counter
5: for  $i \in \{s_{\max}, s_{\max} - 1, \dots, 0\}$  do
6:   if  $T \geq T_{\max}$  then ▷ Exit if reached maximum trials
7:     break
8:   end if
9:    $n_i \leftarrow \lfloor \eta^{s_{\max}-i} \cdot \frac{\eta}{\eta-1} \rfloor$  ▷ Initial configurations
10:   $\mathcal{M} \leftarrow \text{FitRandomForest}(\mathcal{D})$  ▷ Build surrogate model
11:  if  $|\mathcal{D}| = 0$  then
12:     $\Theta_i \leftarrow \text{Sample } n_i \text{ random configurations from } \Theta$ 
13:  else
14:     $\Theta_i \leftarrow \text{Select } n_i \text{ configurations with highest EI based on } \mathcal{M}$ 
15:  end if
16:   $s_i \leftarrow \lfloor \log_{\eta}(\frac{n_i}{1}) \rfloor + 1$  ▷ SH rounds
17:   $\mathcal{A} \leftarrow \Theta_i$  ▷ Set of active configurations
18:   $b \leftarrow b_{\min} \cdot \eta^i$  ▷ Initial budget
19:  for  $l \in \{0, 1, \dots, s_i - 1\}$  do
20:    if  $T \geq T_{\max}$  then ▷ Exit if reached maximum trials
21:      break
22:    end if
23:     $n_{i,l} \leftarrow \lfloor \frac{n_i}{\eta^l} \rfloor$  ▷ Current pool size
24:    for each  $\theta \in \mathcal{A}$  do
25:       $y_{\theta} \leftarrow f(\theta, b)$  ▷ Evaluate configuration
26:       $\mathcal{D} \leftarrow \mathcal{D} \cup \{(\theta, b, y_{\theta})\}$  ▷ Update history
27:       $T \leftarrow T + 1$  ▷ Increment trial counter
28:      if  $b = b_{\max}$  and  $y_{\theta} < y^*$  then
29:         $y^* \leftarrow y_{\theta}, \theta^* \leftarrow \theta$  ▷ Update best
30:      end if
31:      if  $T \geq T_{\max}$  then ▷ Exit if reached maximum trials
32:        break
33:      end if
34:    end for
35:    Sort  $\mathcal{A}$  by performance
36:     $\mathcal{A} \leftarrow \text{Top } \lfloor \frac{n_{i,l}}{\eta} \rfloor \text{ configurations from } \mathcal{A}$ 
37:     $b \leftarrow \min(b \cdot \eta, b_{\max})$  ▷ Increase budget
38:    if  $b = b_{\max}$  or  $|\mathcal{A}| = 1$  then
39:      break
40:    end if
41:  end for
42: end for
43: return  $\theta^*$ 
```

A.5 Evaluation Metrics and details

We evaluate using domain-specific metrics: accuracy for MMLU multiple choice questions based on loglikelihood, zero-shot accuracy for GSM8K and MATH, and Pass@1 for HumanEval and MBPP. We run all evaluations using LM Evaluation Harness[Gao et al., 2024] with vLLM[Kwon et al., 2023] acceleration. For consistency, we use fixed parameters across all tests: batch size 16, temperature 0.0 for greedy decoding, and maximum generation length of 1,024 tokens for GSM8K and 2,048 tokens for other datasets. All experiments run on NVIDIA Tesla A100 GPUs.

A.6 Details of Search Spaces

Within LFS, we define specific parameter ranges for each merging method: Task Arithmetic utilizes task vector weights $\lambda \in [0, 1]$; TIES-Merging combines task vector weights $\lambda \in [0, 1]$ with a ratio to retain parameters $k \in [0.1, 0.99]$; Linear-merging optimizes model coefficients $w_t \in [0, 1]$ subject to $\sum_i w_t = 1$; and Slerp employs an interpolation parameter $t \in [0, 1]$.

A.7 Details of Grid Search on Hyperparameters of base Model Merging Methods

Table 8: Search Ranges of Hyperparameters for Different Model Merging Methods

Merging Methods	Search Ranges of Hyperparameters
Task Arithmetic	Scaling term to merge parameters: $[0.5, 1.0]$
Linear Merging	Scaling term to merge parameters: $[1/n]$ (n : number of models)
TIES-Merging	Scaling term to merge parameters: $[0.5, 1.0]$ Ratio to retain parameters with largest-magnitude values: $[0.5, 0.7, 0.9]$

A.8 Details of search on other Reasoning Tasks

LogiQA is derived from the logical comprehension section of China’s National Civil Servants Examination, specifically designed to evaluate candidates’ critical thinking and problem-solving capabilities. For our search implementation, we utilize the validation dataset with a budget range of 100 – 651.

OpenBookQA is used to measure deep understanding of both subject matter and language comprehension. The dataset comes with an "open book" of fundamental facts. We conducted experiments both with and without facts in the prompt. Our search employs the validation dataset with a budget range of 100 – 500.

PIQA (Physical Interaction: Question Answering) serves as a benchmark dataset for physical commonsense reasoning, with a particular focus on everyday situations and unconventional solutions. We have sampled 1,000 examples from the validation dataset for our search purposes, setting the budget range at 100 – 1,000.

SocialQA stands as a comprehensive benchmark for testing social commonsense intelligence, this dataset evaluates understanding of human actions and their social implications in everyday situations. Our search implementation uses a 1,000-sample subset from the validation data, with a budget range of 100 – 1,000.

MGSM (Multilingual Grade School Math Benchmark) is a benchmark of grade-school math problems. The same 250 problems from GSM8K are each translated via human annotators in 10 languages. We use 1,069 mathematics problems and solutions translated to Japanese from the GSM8K test set by Sakana AI for searching, set a budget range of 100 – 1000.

B Additional Experimental Results.

B.1 Detailed breakdown of performance across specific MMLU categories of GEN-DIS-0 and GEN-DIS-1

Table 9: Performance Comparison on MMLU Subject Categories between LM and GEN-DIS

MMLU Category	LM	GEN-DIS-0	GEN-DIS-1
Social Sciences	62.24	63.24 (+1.00)	63.69 (+1.45)
Humanities	49.52	51.31 (+1.79)	51.09 (+1.57)
STEM	42.82	43.67 (+0.85)	44.37 (+1.55)
Other	61.31	62.66 (+1.35)	62.12 (+0.81)

B.2 Performance comparison of different merging methods in multi-objective optimization.

Table 10: Performance comparison of different merging methods in multi-objective optimization

Method	Model	Src [†]	Srch [‡]	MMLU	GSM8K	MATH	MBPP	HEval	Avg
Multi-Obj (Our)	MULTI-LFS-0	M+C+L	1+2+3	55.03	63.08	11.76	32.60	21.95	36.88 (+5.78)
	MULTI-LFS-1	M+C+L	1+2+3	54.70	66.94	11.38	30.60	23.78	37.48 (+6.38)
	MULTI-LFS-2	M+C+L	1+2+3	54.67	65.13	11.06	30.40	20.73	36.40 (+5.30)
	MULTI-LFS-3	M+C+L	1+2+3	54.99	65.50	9.42	30.20	23.17	36.66 (+5.56)
	MULTI-LFS-4	M+C+L	1+2+3	54.77	66.79	12.06	31.80	24.40	37.96 (+6.86)
Multi-Obj (Task Arith)	MULTI-LFS-0-TA	M+C+L	1+2+3	54.92	62.85	10.62	28.60	18.29	35.06 (+3.96)
	MULTI-LFS-1-TA	M+C+L	1+2+3	54.97	63.07	10.70	31.40	20.12	36.06 (+4.96)
	MULTI-LFS-2-TA	M+C+L	1+2+3	55.46	61.56	10.52	29.80	24.39	36.35 (+5.25)
	MULTI-LFS-3-TA	M+C+L	1+2+3	55.47	63.56	11.36	30.00	20.73	36.26 (+5.16)
	MULTI-LFS-4-TA	M+C+L	1+2+3	54.96	61.48	10.20	29.20	18.29	34.83 (+3.73)
Multi-Obj (Ties)	MULTI-LFS-0-Ties	M+C+L	1+2+3	53.51	63.23	11.64	29.60	20.14	36.62 (+5.52)
	MULTI-LFS-1-Ties	M+C+L	1+2+3	54.62	61.18	10.52	32.00	18.90	35.44 (+4.34)
	MULTI-LFS-2-Ties	M+C+L	1+2+3	54.99	61.56	11.36	30.00	20.73	35.73 (+4.63)
	MULTI-LFS-3-Ties	M+C+L	1+2+3	55.30	62.26	9.86	29.80	18.29	35.10 (+4.00)
	MULTI-LFS-4-Ties	M+C+L	1+2+3	54.24	61.25	10.70	30.20	18.85	35.05 (+3.95)

[†]Src = Source, M+C+L = Math+Code+LM

[‡]Srch = Search, Dataset Index: 1=GSMPlus, 2=MBPPval, 3=MMLUval

HEval = HumanEval, Avg = Average

B.3 Additional result of Budget Distribution

Table 11: Budget Distribution Across Models

Budget	MATH-LFS	CODE-LFS	Multi-LFS	GEN-LFS	GEN-DIS-0	GEN-DIS-1
100	263 (47.2%)	295 (59.0%)	240 (48.0%)	207 (41.4%)	163 (16.3%)	311 (31.1%)
300	152 (30.4%)	205 (41.0%)	161 (32.2%)	181 (36.2%)	165 (16.5%)	307 (30.7%)
1000	85 (17.0%)	-	99 (19.8%)	112 (22.4%)	109 (10.9%)	186 (18.6%)
0	-	-	-	-	563 (56.3%)	196 (19.6%)

C Comparison with evolutionary-based merging

C.1 Similarity

Both studies are hyperparameter optimization-based methods, incorporating layerwise and depthwise modifications—a common strategy in the merging community to maintain architecture stability without post-finetuning Ilharco et al. [2022], Yadav et al. [2024], Yu et al. [2024].

C.2 Difference

However, our method is more effective, which differs in the following three key aspects:

Search Space Design For layerwise search, Akiba et al. [2024] only supports TIES-Merging with uniform layer merging. Ours offers flexibility through multiple merging methods, layer selection, and granular controls. This fine-grained control mitigates layer conflicts and improves performance, as shown in our ablation studies (Table 4). Our experiments reveal that different objectives exhibit varying preferences for merging methods and layer selection.

For depthwise search, Akiba et al. [2024] explores all possible layer interactions, resulting in an excessively large search space that makes it difficult to optimize. Our block-wise design controls the degree of layer interaction through depth granularity, which enables flexible adjustment for different tasks while reducing search space size with fewer hyperparameters (see the Table 12). While our permutation vector P grows exponentially with increasing depth granularity, we have the alternative to replace this by optimizing a learned group of parameters (with the size equal to $M \times D \times R$) and determine the order of layers by sorting its values (the complexity shifts from exponential to linear).

Table 12: Comparison of search space parameters between Evolutionary Search and our approach

Definition	Evolutionary Search Space	Our Approach
L, M	Number of layers/candidate models	
R	Repetition of candidate models	Block-wise layer repetition
D	–	Depth granularity
Layer selection	$2^{L \cdot M \cdot R}$	$2^{M \cdot D \cdot R} \cdot L/D$
Scaling matrix W	$(L \cdot M \cdot R)^2$	L/D
Permutation vector P	–	$L/D \cdot (D \cdot M \cdot R)! / (R!)^{M \cdot D}$ or $M \cdot D \cdot R \cdot L/D$

Objective Compared to Akiba et al. [2024] which only supports single-objective optimization, our study is extended for multi-objective optimization. This is particularly important for large models, as we observe that optimizing for a single objective often leads to improvements in other tasks, demonstrating the inherent multi-task nature of large models. Furthermore, with our multi-objective optimization, our merged models maintain excellent balance across all tasks.

Optimizers Akiba et al. [2024] employs a full-budget, evolution-based optimization, which can be computationally intensive in large search spaces, while our method leverages multi-fidelity evaluation, enabling more effective exploration of the search space. This allows for more trials within the same computational budget while facilitating extensions to more complex multi-objective optimization settings.

Table 13: Configuration parameters of architectures Searched by LFS

Group	Method	Metric	MATH-LFS	GEN-LFS	MULTI-LFS-0	MULTI-LFS-1	MULTI-LFS-2	MULTI-LFS-3	MULTI-LFS-4
Group (1-10)	task_arithmetic	mlp	0.983	-	-	0.303	0.303	0.303	0.293
		att	0.182	-	-	0.948	0.948	0.948	0.881
		other	0.791	-	-	0.997	0.997	0.997	0.997
	linear	mlp	-	[0.118, 0.324, 0.558]	[0.351, 0.344, 0.304]	-	-	-	-
		att	-	[0.430, 0.224, 0.346]	[0.162, 0.298, 0.540]	-	-	-	-
		other	-	[0.317, 0.257, 0.426]	[0.288, 0.371, 0.340]	-	-	-	-
Group (11-20)	task_arithmetic	mlp	0.982	-	0.395	0.395	0.395	0.395	0.395
		att	0.604	-	0.842	0.842	0.842	0.842	0.862
		other	0.329	-	0.300	0.380	0.300	0.300	0.300
	linear	mlp	-	[0.376, 0.258, 0.366]	-	-	-	-	-
		att	-	[0.414, 0.357, 0.229]	-	-	-	-	-
		other	-	[0.263, 0.532, 0.205]	-	-	-	-	-
	slerp(Math, Code)	mlp	0.594	-	-	-	-	-	-
		att	0.566	-	-	-	-	-	-
		other	0.323	-	-	-	-	-	-
Group (21-30)	ties	mlp	-	-	0.778/0.583	0.778/0.583	0.819/0.583	-	0.724/0.583
		att	-	-	0.394/0.312	0.394/0.312	0.373/0.312	-	0.488/0.312
		other	-	-	0.324/0.606	0.349/0.606	0.324/0.606	-	0.371/0.606
	linear	mlp	-	-	-	-	-	[0.4739, 0.4728, 0.0533]	-
		att	-	-	-	-	-	[0.3916, 0.3649, 0.2435]	-
		other	-	-	-	-	-	[0.0342, 0.2826, 0.6832]	-
	slerp(LM, Math)	mlp	0.469	-	-	-	0.113	-	-
		att	0.437	-	-	-	0.339	-	-
		other	0.549	-	-	-	0.58	-	-
Group (31-40)	linear	mlp	-	-	[0.354, 0.382, 0.264]	[0.375, 0.392, 0.234]	-	[0.373, 0.390, 0.237]	[0.354, 0.382, 0.264]
		att	-	-	[0.568, 0.141, 0.292]	[0.556, 0.168, 0.276]	-	[0.562, 0.159, 0.279]	[0.548, 0.156, 0.296]
		other	-	-	[0.344, 0.183, 0.473]	[0.345, 0.183, 0.473]	-	[0.345, 0.183, 0.473]	[0.345, 0.183, 0.473]

Table 14: DIS-Optimized Architecture Parameters for General Reasoning

block	GEN-DIS-0				GEN-DIS-1			GEN-DIS-NR		
	layer_0	layer_1	layer_2	scale	layer_0	layer_1	scale	layer_0	layer_1	scale
1	LM	–	–	1.00	LM	–	0.99	LM	–	1.07
2	Math	–	–	1.00	Base	–	0.78	LM	–	1.00
3	LM	–	–	1.00	LM	–	0.93	LM	–	1.00
4	LM	–	–	1.00	LM	–	1.01	LM	–	1.00
5	LM	–	–	1.00	LM	–	1.00	LM	–	1.00
6	LM	–	–	1.00	LM	–	0.93	LM	–	1.00
7	LM	–	–	1.00	Base	–	1.10	LM	–	1.00
8	LM	–	–	1.00	LM	–	1.00	LM	–	1.00
9	LM	–	–	1.00	LM	–	1.14	LM	–	1.00
10	LM	–	–	1.01	LM	–	1.00	LM	–	1.00
11	LM	–	–	1.00	Base	–	1.00	LM	–	0.97
12	Code	–	–	1.00	LM	–	0.95	LM	–	1.00
13	LM	–	–	1.00	LM	–	0.99	LM	–	1.12
14	LM	–	–	1.00	LM	–	1.00	LM	–	1.00
15	LM	–	–	1.00	LM	–	0.92	LM	–	1.14
16	LM	–	–	1.07	LM	–	0.89	LM	–	0.89
17	LM	–	–	1.00	Base	–	1.00	LM	–	1.00
18	Code	LM	–	1.00	LM	LM	1.00	LM	–	1.00
19	LM	–	–	1.00	LM	LM	1.00	LM	–	1.00
20	Code	–	–	1.00	LM	–	1.00	LM	–	1.00
21	Base	–	–	1.00	Base	–	1.00	–	–	1.15
22	LM	–	–	1.00	LM	–	1.00	LM	–	1.00
23	Math	LM	–	1.00	LM	–	1.00	LM	–	1.04
24	Base	–	–	1.00	LM	LM	1.00	LM	–	1.00
25	Code	LM	–	1.00	LM	–	1.00	–	–	1.00
26	Base	–	–	1.00	LM	–	1.00	–	–	0.93
27	Base	–	–	1.05	LM	–	1.05	LM	–	1.00
28	Math	LM	–	1.00	LM	LM	1.00	LM	LM	1.06
29	LM	–	–	1.07	LM	–	1.00	LM	–	1.00
30	Math	LM	–	0.87	LM	LM	1.00	LM	–	1.21
31	Base	–	–	1.00	LM	LM	1.00	LM	LM	1.00
32	Math	LM	–	1.00	LM	–	1.05	LM	–	1.10
33	LM	–	–	1.00	Base	–	1.00	LM	LM	0.99
34	LM	–	–	1.00	LM	LM	1.00	LM	–	1.00
35	LM	–	–	1.00	LM	–	1.00	LM	–	1.08
36	LM	–	–	1.20	Base	–	1.00	LM	–	1.07
37	Base	–	–	1.00	LM	–	1.13	LM	LM	1.32
38	Code	–	–	1.00	LM	–	1.03	LM	LM	1.00
39	Math	LM	–	1.00	LM	–	1.00	LM	–	1.00
40	Code	–	–	1.00	LM	–	1.01	LM	–	1.00

Table 15: DIS-Optimized Architecture Parameters for OpenbookQA

block	OpenbookQA				OpenbookQA+F			
	layer_0	layer_1	layer_2	scale	layer_0	layer_1	layer_2	scale
1	LM	–	–	1.00	Base	–	–	0.96
2	Code	–	–	1.00	Code	LM	–	1.00
3	LM	–	–	1.00	LM	–	–	1.00
4	LM	–	–	1.00	LM	–	–	0.97
5	LM	–	–	1.06	LM	Code	–	1.00
6	LM	–	–	1.00	Base	–	–	1.00
7	LM	–	–	1.00	Base	–	–	1.00
8	Math	LM	–	1.00	LM	–	–	1.19
9	LM	–	–	1.00	Code	–	–	1.00
10	LM	–	–	1.00	LM	–	–	1.00
11	LM	–	–	1.00	Math	–	–	1.00
12	Base	–	–	1.00	Base	–	–	1.00
13	LM	–	–	1.00	LM	–	–	0.91
14	LM	–	–	1.00	Base	–	–	1.00
15	LM	–	–	1.00	LM	–	–	1.08
16	LM	–	–	1.00	LM	–	–	1.00
17	LM	–	–	1.00	LM	–	–	0.99
18	LM	–	–	0.85	LM	–	–	1.00
19	LM	–	–	1.00	LM	–	–	1.00
20	LM	–	–	1.00	Code	–	–	1.07
21	LM	–	–	1.00	Base	–	–	1.21
22	LM	–	–	1.00	LM	–	–	0.98
23	LM	–	–	1.00	Code	–	–	1.00
24	LM	–	–	1.00	Base	–	–	0.92
25	Code	LM	–	1.00	LM	–	–	1.00
26	Base	–	–	1.00	LM	–	–	0.93
27	Code	LM	–	1.00	Math	LM	–	1.08
28	Code	LM	–	0.96	Code	–	–	1.18
29	LM	–	–	1.00	LM	–	–	1.00
30	Math	LM	–	1.00	Code	LM	–	1.01
31	LM	–	–	1.00	LM	–	–	0.89
32	LM	–	–	1.00	Base	–	–	1.05
33	LM	–	–	1.00	LM	–	–	1.00
34	LM	–	–	1.00	Math	LM	–	0.83
35	LM	–	–	1.00	Code	LM	–	1.12
36	LM	–	–	1.20	LM	–	–	1.00
37	LM	–	–	1.00	Math	–	–	1.13
38	LM	–	–	1.00	LM	–	–	1.03
39	LM	–	–	1.00	Math	–	–	1.00
40	LM	–	–	1.00	Base	–	–	1.01

Table 16: DIS-Optimized Architecture Parameters for MGSM_JA

block	MGSM_JA_0				MGSM_JA_1		
	layer_0	layer_1	layer_2	scale	layer_0	layer_1	scale
1	Base	—	—	0.99	Math	—	0.98
2	Math	—	—	1.00	Base	—	1.12
3	Math	—	—	0.96	LM_JA	—	1.00
4	Math	—	—	1.00	Base	—	1.00
5	Math	—	—	1.00	Math	LM_JA	1.00
6	Math	—	—	1.00	Math	—	0.93
7	Math	LM	—	1.00	Math	—	1.00
8	Math	—	—	1.11	Math	—	1.00
9	Math	LM	—	1.00	Math	—	1.00
10	Math	—	—	1.10	Math	LM_JA	1.00
11	Math	—	—	1.00	LM_JA	—	1.00
12	Math	LM	—	1.06	Math	LM_JA	1.00
13	LM	Math	—	1.00	Math	—	1.00
14	LM	Math	—	0.83	Math	—	0.97
15	Math	—	—	0.86	Base	—	1.00
16	Math	—	—	1.00	Base	—	0.99
17	Code	—	—	1.00	Math	—	1.09
18	Math	—	—	1.00	Math	—	1.00
19	Base	—	—	1.00	Base	—	0.90
20	Math	—	—	1.00	Math	—	1.26
21	Base	—	—	1.00	Base	—	1.24
22	Base	—	—	1.00	Base	—	1.00
23	Math	—	—	0.96	Math	—	0.82
24	Base	—	—	0.85	Math	—	1.08
25	Math	—	—	1.01	Base	—	1.00
26	Code	—	—	1.00	Base	—	1.00
27	Math	—	—	1.00	LM_JA	—	1.00
28	Math	—	—	1.00	Math	—	1.07
29	Math	—	—	1.00	Base	—	1.00
30	Base	—	—	1.00	LM_JA	Math	0.87
31	Code	—	—	1.04	Math	LM_JA	0.84
32	Math	LM	—	0.89	Math	LM_JA	0.99
33	Math	—	—	1.00	Math	—	1.00
34	Base	—	—	1.00	Math	LM_JA	0.73
35	LM	—	—	1.00	Math	—	1.00
36	Math	—	—	0.98	LM_JA	—	1.00
37	Math	—	—	1.00	Math	—	1.00
38	Base	—	—	1.00	Math	LM_JA	1.00
39	Math	—	—	0.95	Math	—	1.00
40	Base	—	—	1.00	Math	—	1.00